2021 43rd Annual International Conference of the
IEEE Engineering in Medicine & Biology Society (EMBC)
Oct 31 - Nov 4, 2021. Virtual Conference

Measurement of Tremor on Arteriovenous Fistulas with a Flexible Capacitive Sensor

Kan Luo[1], Cong Cai[1], Zhichen Lai[1], Bingfa Huang[1], Jiansheng Cai[2], Chaobing Liang[1], Jianxing Li[1]

Abstract— **Arteriovenous fistula (AVF) is a widely used vascular access for hemodialysis in clinical. It is a great challenge to monitoring the status of AVF in daily life due to acute AVF stenosis may occur on unnoticeable occasions, such as sleeping. Inspiring tremor is almost always accompanied by a healthy AVF, which can be adopted as an essential physiological sign for AVF monitoring. Hence, a fistula tremor measurement system based on a flexible capacitive pressure sensor is designed in this study. The sensor consists of polydimethylsiloxane(PDMS) dielectric layers, electrode layers, ground layers, and shielding layers. The PDMS layers are fabricated as cross superposition transverse microstructure film to enhance dielectric constant and sensitivity of the sensor. The isolation shielding layers and ground layers guarantee the sensing chain is noise-free. A microcontroller embedded AD7746 measurement circuit is designed for signal acquisition. We test our prototype on the wrists of healthy volunteers and AVF on dialysis patients separately. The pulse signals and AVF tremor signals are clear and distinguishable. The sensor and measurement system have excellent potential in wearable AVF monitoring.**

I. Introduction

Chronic kidney disease (CKD) has become a global public health problem, characterized by high prevalence and high mortality. Studies have shown that the number of CKD patients reached 697.5 million worldwide in 2017, of which 0.77% were patients with end-stage renal disease (ESRD) [1]. Hemodialysis is the most commonly used treatment to maintain the survival of ESRD patients. In order to perform hemodialysis, a forearm artery needs to be surgically connected to an adjacent vein to form an arteriovenous fistula (AVF). The patient's own physiological factors, poor vascular conditions, or inadvertent compression of AVF in daily life may cause AVF to undergo thromboembolism. For patients with thrombosis, clinical treatment methods such as local thrombolysis and fistula removal can be used to recanalize AVF. The shorter the embolism is, the higher the possibility of AVF recanalization [2]. Therefore, it is of great clinical significance to monitor the status of AVF for a long time and detect thromboembolism in time.

The commonly used medical tests for AVF are angiography and Doppler ultrasound. Angiography is the gold standard for the assessment of AVF, but it requires the injection of contrast agents, which is risky for patients and should not be done too many times [3-4]. Although Doppler ultrasound is of low-risk, it can only be performed by medical professionals to avoid large human errors. Both methods require expensive equipment and professional operators and are not suitable for home care or wearable applications. In addition, a healthy AVF has both tremor and murmur physiological characteristics, and an experienced healthcare professional can determine whether an AVF is embolic by palpation or stethoscope.

In addition to detecting AVF by large devices such as Doppler ultrasound, some scholars have assessed the status of AVF by photoplethysmography (PPG). J. X. Wu et al [5] and Y. C. Du et al [6] proposed the feasibility of measuring the degree of AVF stenosis by PPG signals from patients' hands. P. Chiang et al [7] designed a novel blood flow sensor based on PPG principle and calibrated it by neural network. In addition, some other scholars have started their research on the acoustic special diagnostic signal of AVF. W. L. Chen et al [8] proposed a screening system for AVF stenosis assessment based on fractional-order fuzzy Petri nets. H. Y. Wang et al [9] used a homemade wireless blood flow sound recorder combined with a two-dimensional feature pattern built based on s-transform to predict AVF stenosis. T. Tong et al [10] designed a portable wireless endovascular murmur acquisition system and analyzed time-domain waveform features to diagnose endovascular obstruction.

On the other hand, tremor is also an important feature of AVF, and the signal is mixed in the pulse wave signal of AVF. In recent years, many scholars have used flexible capacitive sensors for the measurement of physiological signals, but fewer have used them for the measurement of AVF tremor. S. Chen et al [11] prepared a porous polydimethylsiloxane (PDMS) film, and the resulting sensor showed excellent performance in both wrist artery pulse and plantar pressure monitoring. B. Zhuo et al [12] used a 3D-printed mold to fabricate the dielectric layer of a capacitive sensor, and the resulting sensor was able to reliably monitor weak human physiological signals in real time. Using flexible capacitive pressure sensors to measure AVF tremor is not as easy to be affected by ambient lighting as PPG sensor, nor is it easy to have certain requirements for ambient sound like sound acquisition. Therefore, in this study, a flexible capacitive pressure sensor is used to measure the AVF tremor.

This paper is organized as follows: in section 2, the structure of the measurement system and the manufacturing process of the capacitive sensor are introduced. In Section 3, the performance of the measurement system is tested first, including sensitivity test and frequency response test. It was then used to measure the wrist pulse of healthy volunteers and

This work was supported by: Grant 2018J01639, 2020J01876 from the Natural Science Foundation of Fujian Province, Grant 61601124 from the NSFC, Grant GY-Z17161, 160058 from the Research Foundation of Fujian University of Technology.

1. Kan Luo, Cong Cai, Zhichen Lai, Bingfa Huang, Chaobing Liang, Jianxing Li are with the Fujian University of Technology, Fuzhou, 350118, China (phone: 0086-17720815348; e-mail: luokan@fjut.edu.cn).
2. Jiansheng Cai is with Zhangzhou Hospital of traditional Chinese Medicine, Zhangzhou, 363000, China. (e-mail: cjsh5588@126.com).

the AVF of dialysis patients, and the measured normal pulse signal were compared with the AVF signal. In the last section, this paper is summarized.

II. Material and Method

A. AVF Tremor Measurement System

The AVF tremor measurement system is shown in Fig. 1(a), which mainly consists of a flexible capacitive pressure sensor and a capacitance measurement device. The capacitance measurement device consists of a capacitance detection circuit, a data transmission circuit, a voltage conversion circuit, and a microprocessor. The capacitance detection circuit uses a digital capacitance converter (AD7746, Analog Devices) with resolution of up to 4aF. The system uses a Micro USB cable to connect directly to a computer. In addition to data transmission, the computer also provides power for the measurement system. A voltage conversion circuit (TPS73033, Texas Instruments) regulates the supply voltage from 5 V to 3.3 V. In addition, a microcontroller (STM32G030C8T6, STMicroelectronics) and a USB converter chip (CH340E, Nanjing Qinheng Microelectronics) are used for data processing and data transmission.

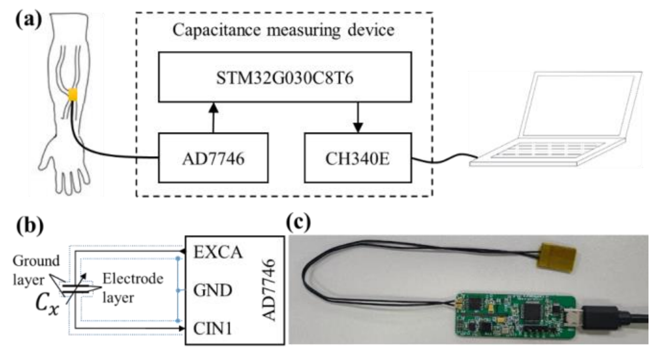

Fig. 1. (a) Block diagram of the measurement system. (b) Schematic diagram of the AD7746 capacitance measurement circuit. (c) Physical diagram of the measurement system.

In order to improve the anti-interference capability, the capacitive pressure sensor is connected to the capacitance measurement device by a shielded line. As shown in Fig. 2(b), the EXCA pin and CIN1 pin of the AD7746 are connected to the two electrode layers of the capacitive pressure sensor, and the two ground layers of the sensor are connected to the GND of the AD7746 through the shield layer of the shielded line. When the system is in measurement mode, the EXCA pin outputs a square wave excitation signal with a fixed frequency of 32 KHz, and then the capacitance value of the sensor is obtained by detecting the CIN1 channel. When the AD7746 is in single-ended input mode, the compensation register can be configured to enable the measurement range from 0pF to 8.192pF. The data is then processed and transferred to a computer for recording and display via CH340E.

B. Fabrication of the Flexible Capacitive Pressure Sensor

The fabrication of the flexible capacitive pressure sensor is shown in Fig. 2(a). First, a PDMS mold with parallel microgrooves on the surface is fabricated by a 3D-printer using acrylonitrile butadiene styrene (ABS) material, as shown in Fig. 2(c). The size of the mold is 30 mm × 30 mm, and the parallel microgrooves are 100μm deep and 200μm wide, and the microgrooves are separated by 400μm. The width of the microgrooves is limited by the accuracy of the 3D-printer. The smaller the width, the more susceptible the micropillars on the PDMS film to be deformed by force and the higher the sensitivity of the sensor. Then the PDMS master agent and the curing agent (Sylgard 184, Dow Corning) are mixed thoroughly with a ratio of 10:1 and left to stand for 10 minutes. The PDMS mixture is poured into the cleaned and sprayed mold with release agent (HAMLD, 184) and scraped flat, and then degassed in a vacuum chamber for 10 minutes. After degassing, the mold is removed without air bubbles and cured at 80°C for 2 hours. After curing, the whole PDMS film is removed from the edge with flat-tipped tweezers and cut into 10 mm×10 mm films with microstructures. Finally, the two PDMS films are laminated face-to-face so that the microstructure slots are cross-laminated together and assembled with the other layers of the prepared sensor.

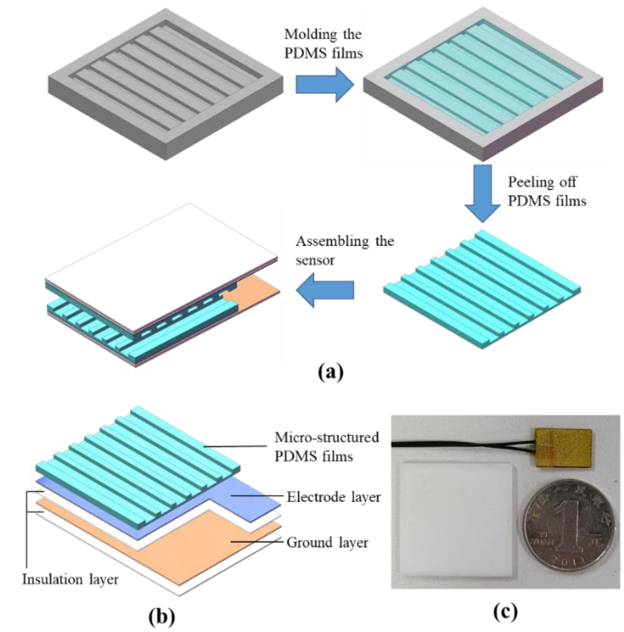

Fig. 2. (a) Manufacturing process of the flexible capacitive pressure sensor. (b) Pole plate structure of a single sensing pole plate. (c) 3D-printed PDMS mold and flexible capacitive pressure sensor physical diagram.

The flexible capacitive pressure sensor is composed of two sensing plates. The structure of a single sensing plate is shown in Fig. 2(b), which is mainly composed of the conductive layer, the insulating layer and a PDMS film layer. The conductive layer contains two layers, the electrode layer and the ground layer, both of which are made of conductive cloth (mainly made of red copper wire, with adhesive on one side and conductive on both sides). To avoid short-circuiting between the layers and to protect the whole plate, an insulating layer (polyimide insulating tape, thickness is 0.055 mm) is placed between the electrode layer and the ground layer, as well as on the outward-facing side of the plate. Before assembly, the required layers are prepared in advance. Take a single sensing pole plate as an example, the electrode and ground layers are cut from the conductive tape, and the corresponding two insulation layers are cut from the polyimide insulation tape. The extended part of the electrode layer that is not in contact with the PDMS film is used to connect the signal layer of the shield. The grounding layer has a larger area than the electrode layer, and the uncovered part of it is used to connect the shield layer of the shielded line. During fabrication, the insulation layer - ground layer - insulation layer - electrode layer - PDMS film layer are laminated sequentially, and then the two sides of the manufactured sensing pole plate are assembled together. The final flexible capacitive pressure sensor is shown in Fig. 2(c), with a size of 14 mm×10 mm and thickness of only 1.3 mm. The effective sensing size of the sensor is 10 mm×10 mm.

III. Experiments and Results

In this experiment, if not specified, the size of the flexible capacitive pressure sensor is 14mm×10mm, and the effective sensing size is 10mm×10mm, and it is connected to the capacitance measurement device through a 200mm long shielded wire.

A. Performance Test Experiment

In the sensitivity test experiment, an ultra-thin glass sheet of size 10 mm × 10 mm is placed on the effective sensing area of the sensor, and a pressure (P) is applied to the sensor by means of a weight on the glass sheet. The pressure sensitivity is defined as:

$$s = \Delta(\Delta C / C_0) / \Delta P \tag{1}$$

Where: $\Delta C/C_0$ is the relative capacitance change of the sensor, and ΔC is the change in capacitance value measured by the sensor relative to C_0 when pressure is applied. In this study, C_0=1.738pF.

The measured relationship between $\Delta C/C_0$ and P is shown in Fig. 3(a), and the slope of this measurement curve is the pressure sensitivity s. The sensitivity of the sensor is 0.35 kPa^{-1} when the pressure is less than 1 kPa, and when the pressure increases to 4 kPa, the sensor still has a sensitivity of 0.11 kPa^{-1}. Because AVF receives too much pressure, it is easy to block the fistula and produce thrombus, and the tremor signal of AVF is weak. Therefore, the sensor should work in the low-pressure region (0-1kPa) with high sensitivity, in

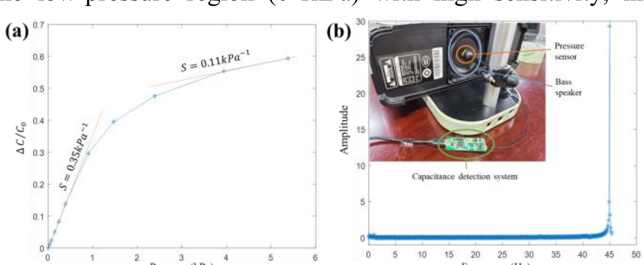

Fig. 3. Performance test experiment. (a) The measured relationship between $\Delta C/C_0$ and P. (b) Frequency response test spectrum of sensor under 45Hz sound signal.

which the actual change in measured capacitance value (0.006pF) is greater than the effective resolution of the capacitance measurement device for every 10Pa (0.1g) change in applied pressure.

The tremor of AVF can be shown as a rapidly changing force. In order to prevent measurement errors, it is necessary to test the frequency response of the tremor measurement system. In this study, a subwoofer is used to measure the frequency of the sensor. As shown in Fig. 3(b), the sensor is in contact with the diaphragm of the subwoofer through a bracket, allowing the speaker to play a sound signal of a fixed frequency. Gradually change the frequency of the sound from low to high, and adjust the volume so that the diaphragm vibration of the loudspeaker is roughly the same as the actual tremor touch of the AVF. The capacitance signal of the sensor is measured by the capacitance measuring device, and its frequency spectrum is analyzed. The maximum sensor frequency response obtained from the test is 45Hz, which is the upper limit of the frequency detection of the capacitance measurement system and meets the requirements of the capacitance measurement system.

B. Measurement Comparison Experiment.

In order to verify that the tremor measurement system designed in this study can measure the AVF tremor signal of

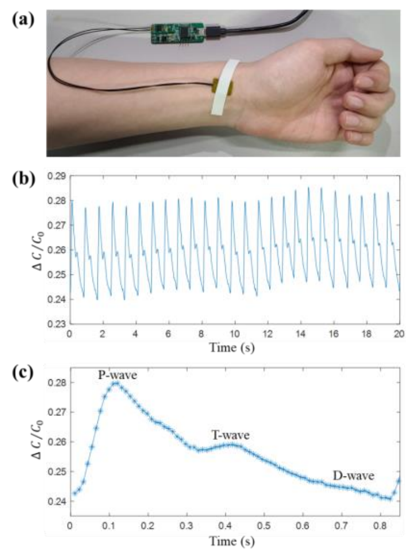

Fig. 4. (a) Tremor measurement system is used to measure the wrist pulse of healthy volunteers. (b) Wrist pulse measurement signal. (c) A segment of wrist pulse measurement signal.

dialysis patients, the wrist pulse signals of healthy volunteers were measured. In cooperation with Zhangzhou Hospital of traditional Chinese Medicine, the AVF of dialysis patients was also measured.

As shown in Fig. 4(a), the sensor is attached to the wrist of healthy volunteers with medical cotton tape. Fig. 4(b) shows the measured wrist pulse signal, and Fig. 4(c) shows a segment of the measured signal. It can be seen from the figure that the tremor measurement system can clearly detect complete pulse waveform of healthy volunteers, and can also distinguish the main wave (P-wave), tidal wave (T-wave) and repulse wave (D-wave) in the pulse signal.

As shown in Fig. 5(a), the sensor is attached to the AVF of a dialysis patient with medical cotton tape. Fig. 5(b) shows the AVF measurement signal, and Fig.5 (c) shows a segment of the measurement signal. Compared with the wrist pulse signal of healthy volunteers in Fig. 4(c), it can be clearly seen on Fig. 5(c) that the AVF measurement signal is a tremor signal superimposed on a normal pulse wave signal, which is the signal to be detected in this study. Furthermore, five dialysis

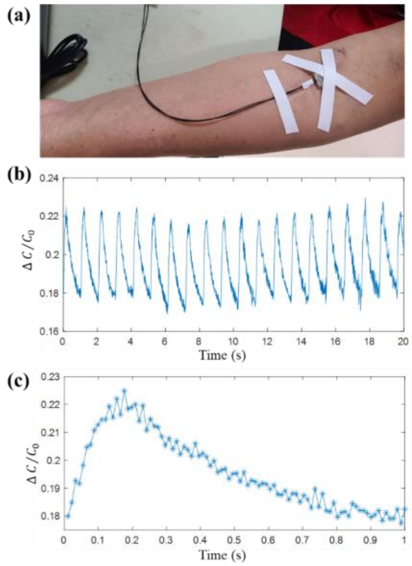

Fig. 5. (a) The tremor measurement system is measured on the AVF of dialysis patients. (b) AVF measurement signal. (c) A segment of AVF measurement signal.

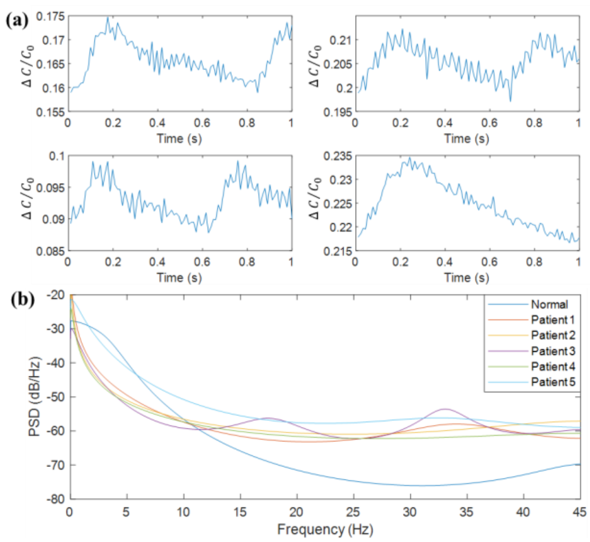

Fig. 6. (a) The AVF measurement signals of the remaining four patients. (b) Power spectral density curves of the signals of a healthy volunteer and five dialysis patients.

patients were tested in this study. Except for the results of patient #1 presented in Fig. 5, AVF measurement signals of the remaining four patients are shown in Fig. 6(a). Fig. 6 (b) are the power spectral density (PSD) curves of the AVF signals from a healthy volunteer and the five dialysis patients. It can be found that distinguished characters appear in the range above 20 Hz, with the PSD of the healthy volunteer's pulse signal less than -70dB while the AVF measurement signals from the dialysis patients staying at -60dB between 25Hz-40Hz.

IV. Conclusion

In this study, a fistula tremor measurement system based on a flexible capacitive pressure sensor was designed. The dielectric layer of the sensor is composed of two layers of PDMS films with a transverse microstructure. The design of the outermost layer of the sensor and the adoption of a shielding line improve the anti-interference ability of the system. The final sensor not only keeps flexibility, but also has high sensitivity, and its response frequency can reach the upper limit of the detection frequency of the capacitance measuring device. In the measurement comparison experiment, wrist pulse signals of healthy volunteers and AVF signals of dialysis patients are collected. The waveforms, frequency spectrum and power spectral density of the two kinds of measured signals are compared, and the results show that there is a great distinction between the two kinds of signals. Measuring the tremor of AVF using a flexible capacitive pressure sensor has the advantages of low power consumption, high detection sensitivity and low risk for patients. This method can be used to perform long-time real-time monitoring of AVF dialysis patients and has a broad application prospect.

References

[1] B. Bikbov, C. A. Purcell, A. S. Levey et al, "Global, regional, and national burden of chronic kidney disease, 1990–2017: a systematic analysis for the Global Burden of Disease Study 2017," *The Lancet*, vol. 395, no. 10225, pp. 709-733, 2020.

[2] H. K. Kim, T. W. Kwon, Y. P. Cho et al, "Outcomes of Salvage Procedures for Occluded Autogenous Radiocephalic Arteriovenous Fistula," *Therapeutic Apheresis and Dialysis*, vol. 15, no. 5, pp. 448-453, 2011.

[3] C.-Y. Ye, "Functional evaluation of vessel access," *Chinese Journal of Blood Purification*, vol. 6, no. 7, pp. 361-364, 2007.

[4] J. Ji, X.-Q. Ding, X.-H. Xu et al, "Effect of the low-osmolality nonionic contrast media on renal function in patients undergoing coronary intervention: a prospective study," *Chinese Journal of Nephrology*, vol. 22, no. 7, pp. 388-392, 2006.

[5] J. X. Wu, C. H. Lin, M. J. Wu et al, "Bilateral photoplethysmography analysis for arteriovenous fistula dysfunction screening with fractional-order feature and cooperative game-based embedded detector," *Healthcare technology letters*, vol. 2, no. 3, pp. 64-69, 2015.

[6] Y. C. Du and A. Stephanus, "A Novel Classification Technique of Arteriovenous Fistula Stenosis Evaluation Using Bilateral PPG Analysis," *Micromachines*, vol. 7, no. 9, pp. 147, 2016.

[7] P. Chiang, P. C.-P. Chao, D. Tarng and C. Yang, "A Novel Wireless Photoplethysmography Blood-Flow Volume Sensor for Assessing Arteriovenous Fistula of Hemodialysis Patients," *IEEE Transactions on Industrial Electronics*, vol. 64, no. 12, pp. 9626-9635, 2017.

[8] W. L. Chen, C. D. Kan and C. H. Lin, "Arteriovenous Shunt Stenosis Evaluation Using a Fractional-Order Fuzzy Petri Net Based Screening System for Long-Term Hemodialysis Patients," *Journal of Biomedical Science and Engineering*, vol. 7, no. 5, pp. 258-275, 2014.

[9] H. Y. Wang, C. H. Wu, C. Y. Chen et al, "Novel Noninvasive Approach for Detecting Arteriovenous Fistula Stenosis," *IEEE Transactions on Biomedical Engineering*, vol. 61, no. 6, pp. 1851-1857, 2014.

[10] T. Tong, L. Qiu, J. Zhong et al, "Wearable Arteriovenous Fistula Murmur Monitoring System Based on Embedded Wi-Fi Technology," in *2018 IEEE SmartWorld, Ubiquitous Intelligence & Computing, Advanced & Trusted Computing, Scalable Computing & Communications, Cloud & Big Data Computing, Internet of People and Smart City Innovation (SmartWorld/SCALCOM/UIC/ATC/CBDCom/IOP/SCI)*, Guangzhou,

[11] S. Chen, B. Zhuo and X. Guo, "Large Area One-Step Facile Processing of Microstructured Elastomeric Dielectric Film for High Sensitivity and Durable Sensing over Wide Pressure Range," *ACS Applied Materials and Interfaces*, vol. 8, no. 31, pp. 20364-20370, 2016.

[12] B. Zhuo, S. Chen and M. Zhao et al, "High Sensitivity Flexible Capacitive Pressure Sensor Using Polydimethylsiloxane Elastomer Dielectric Layer Micro-Structured by 3-D Printed Mold," *IEEE Journal of the Electron Devices Society*, vol. 5, no. 3, pp. 219-223, 2017.